Caspase-dependent activation of Hedgehog-signalling sustains proliferation and differentiation of ovarian somatic stem cells.

Alessia Galasso[1], Daria Iakovleva[1], Luis Alberto Baena-Lopez[1]*

* Author for correspondence

1: Sir William Dunn School of Pathology. University of Oxford. South Parks Road. Oxfordshire, UK. OX13RE

Key words:

ABSTRACT

There is increasing evidence associating the role of caspases with the regulation of basic cellular functions beyond apoptosis. However, the molecular interplay between these enzymes and the signalling networks active in non-apoptotic cellular scenarios remains largely uncharacterized. Here, we show that transient and non-apoptotic caspase activation facilitates Hedgehog-signalling in *Drosophila* and human ovarian cells with a somatic origin. Importantly, this novel caspase function controls gene expression, cell proliferation, and differentiation. We also molecularly link this uncovered caspase role with the fine regulation of the Hedgehog-receptor, Patched. Altogether, these findings strikingly suggest that caspase activation can act as a pro-survival factor that promotes the expansion and differentiation of normal healthy cells. These observations have profound implications on our understanding of caspase biology from a cellular, physiological and evolutionary perspective.

MAIN

The transient and moderate activation of caspases in specific subcellular compartments is essential for the regulation of a diverse range of cellular functions beyond apoptosis[1-4]. However, the molecular details underlying these non-apoptotic functions are largely unknown in many cellular scenarios. Addressing this question can provide essential information to fully understand caspase biology, as well as the physiological role of these enzymes in a wide variety of cells, including stem cells.

During the last decade, the adult *Drosophila* ovary has been extensively used to investigate stem cell physiology and intercellular communication[5, 6]. Additionally, it is one of the cellular models that shows widespread non-apoptotic caspase activation in response to environmental stress[7]. Therefore, it appears to be an ideal cellular system to study the interplay between caspases, signalling mechanisms, and stem cell physiology. The early development of *Drosophila* female gametes occurs in a cellular structure referred to as the germarium. The germarium is formed by the germline and the surrounding somatic cells[5, 6] (Figure. 1a). One of the main genetic cascades coordinating the physiology of somatic and germinal cells is the Hedgehog-signalling pathway[8-14]. The interaction of the Hedgehog (Hh) ligand with its membrane receptor Patched (Ptc) allows the activation of the signalling transducer Smoothened (Smo)[15]. This ultimately prevents the proteolytic processing of the transcriptional regulator Cubitus interruptus (Ci)[15], thus eliciting the activation of multiple target genes[15]. The main somatic Hh-activating cells in the germarium are the escort cells[12] and the follicular stem cells[13] (Fig. 1a). Hh-pathway activation in the escort cells controls the signals that emanate to the germline[9, 12]. This remote system of signalling modulates the timely differentiation of the germline[9, 12]. In the follicular stem cells, Hh-pathway activation promotes cell proliferation and cell differentiation[11, 14, 16, 17], while Hh-deficiency has the opposite effect[8, 11, 13]. Importantly, the pro-proliferative role of Hh-signalling in ovarian somatic cells is evolutionarily conserved[18-20]. Furthermore, while an increase in Hh-signalling stimulates tumour growth and metastatic behaviour of ovarian somatic malignancies[20, 21], its downregulation through chemical agents or genetic factors compromises cell division and differentiation[19, 21, 22].

Our work shows that non-apoptotic caspase activation in somatic cells of the *Drosophila* germarium modulates Hh-signalling, autophagy, and the cellular properties of ovarian somatic cells. We also molecularly connect this unexpected

caspase functions with the fine-tuning of Ptc levels. Finally, our findings suggest that the caspase-dependent effects on Hh-signalling and autophagy are evolutionarily conserved in human ovarian cells with somatic origin. Altogether, these observations uncover unknown features of caspase biology, whilst conferring a pro-survival role to these enzymes in the ovary.

RESULTS

Non-apoptotic Dronc activation in ovarian somatic stem cells

We recently generated a novel caspase sensor based on a cleavable, but catalytically inactive version of the effector caspase, *Drice* (Drice based sensor QF; DBS-S-QF)[23]. Among other applications, this sensor can be used to induce the expression of multiple fluorescent markers with variable perdurance in caspase-activating cells[23]. This feature is able to provide a short-term perspective of caspase activation dynamics, as well as a permanent labelling of caspase-activating cells in *Drosophila* tissues[23]. Since it has been shown that strong environmental stress (starvation and cold shock) can induce widespread non-apoptotic caspase activation in the *Drosophila* ovary[7], we sought to investigate whether under moderate stress such activation could exist and follow a stereotyped pattern. The detailed inspection of adult flies maintained at 29 ^{o}C showed discrete subsets of escort and follicular cells labelled with the short-lived fluorescent markers induced by our caspase sensor (Fig. 1b). Interestingly, marked cells did not always show signs of cell death such as DNA fragmentation (green positive cells and TUNEL negative in Fig.1b). Furthermore, they often displayed only the fluorescent signature of caspase activation in the past (green signal, Fig. 1b), but not the marker of ongoing caspase activation at the time of dissection (red signal, Fig. 1b). Confirming the presence of transient caspase activation in healthy and proliferative cells, large groups of follicular cells including the follicular stem cells and escort cells were permanently labelled with the DBS-S-QF caspase sensor (Fig. 1c). Furthermore, the number of enduringly labelled germaria with this system increased over time (from 8% to 22% in ovaries dissected at 7 and 14 days after adult eclosion, respectively; Fig. 1d). These results demonstrated the presence of transient and non-apoptotic caspase activation in somatic cells of the germarium, including the proliferative stem cell precursors, under moderate stress.

Since DBS-S-QF was designed to specifically report the activation of initiator caspases[23], and *Dronc* (the *Drosophila* orthologue of the mammalian caspase-9) is the main initiator *Drosophila* caspase associated with non-apoptotic functions, we sought to investigate its transcriptional regulation in the ovary by using a *Dronc*$^{KO\text{-}Gal4}$ strain generated in the laboratory that recapitulates physiological expression of this gene[24]. *Dronc*$^{KO\text{-}Gal4}$ was able to drive the expression of a UAS-Histone-RFP transgene in the escort and follicular cells of the germarium at 29°C (Fig. 1e, f). This expression pattern was also confirmed through cell lineage-tracing experiments using the same Gal4 driver (Fig. 1g). This data strongly suggested that *Dronc* could be responsible for the caspase activation patterns observed with DBS-QF sensor (compare Fig. 1c, 1f and 1g).

Dronc acts as a pro-survival factor that sustains follicular stem cell functions

To determine the biological relevance of caspase activation in the germarium, we took advantage of a conditional allele of Dronc generated through genome engineering protocols[24, 25]. This allele contains a wild-type *Dronc* cDNA flanked by FRT recombination sites followed by a transcriptional activator QF (hereafter *Dronc*$^{FRT\text{-}Dronc\text{-}FRT\text{-}QF}$)[24]. To test the excision efficiency of the *Dronc* FRT-rescue cassette, we expressed flippase recombinase within the escort and follicular stem cells under the regulation of c587-Gal4[26] (Supplementary Fig. 1a). The excision of the cassette allowed the activation of the transcriptional QF factor under the physiological regulation of the *Dronc* promoter, and the subsequent activation of a GFP marker (QUAS-CD8-GFP) within the somatic cells transcribing *Dronc* in all of the analysed germaria (n=20; Supplementary Fig. 1b). These experiments confirmed the transcriptional patterns of *Dronc* in the germarium, whilst demonstrating the suitability of our conditional allele to efficiently target *Dronc* expression in different somatic cell populations, including those with low rates of proliferation (e.g. escort cells). Combining this allele with the 109-30-Gal4 driver, we next preferentially removed *Dronc* expression in the follicular stem cells and their progeny[13] (Supplementary Fig. 1c). This genetic manipulation reduced the expression of the somatic marker Castor (Fig. 2a and 2b), the number of follicular cells, and the size of the 2b region of the germarium (Supplementary Fig. 1 d-e). Additionally, we noticed that these genetic manipulations facilitated the expansion of the area in the germarium occupied by Orb-positive cells (germline cells; Fig. 2c and 2d). These initial results indicated the ability of Dronc to regulate the cellular properties of somatic stem cells and the germline in the germarium. In a complementary set of experiments, we preferentially targeted the expression of *Dronc* in escort cells using

the *spitz*-Gal4 driver (Supplementary Figure 1f). Castor expression was almost unaffected by these genetic manipulations (Fig. 2b, e), and was only reduced when the *spitz*-Gal4 driver was expressed in follicular stem cells (Supplementary Fig. 1g). However, *Dronc* deficiency in the escort cells led to a pronounced expansion of the germline (Orb-positive cells, Fig. 2d, f). The simultaneous elimination of *Dronc* expression in escort and follicular cells using c587-Gal4 recapitulated all the aforementioned phenotypes in somatic cells and the germline (Castor downregulation and Orb expansion; Figure 2b, d). Confirming the specificity of our results with *Dronc* expression, equivalent results were obtained using a different conditional allele, which expressed a Suntag-HA-Cherry chimeric protein instead of QF upon the FRT-rescue cassette excision ($Dronc^{KO\text{-}FRT\ Dronc\text{-}GFP\text{-}Apex\ FRT\text{-}Suntag\text{-}HA\text{-}Cherry}$ [24], Fig. 2g). Furthermore, the overexpression of a *Dronc*-RNAi construct under the regulation of $Dronc^{KO\text{-}Gal4}$ generated a comparable, but less penetrant, version of the described phenotypes (Supplementary Fig. 1h, i). Together this data confirmed that the non-apoptotic activation of Dronc can act as a pro-proliferative and pro-differentiating factor in the follicular stem cells. Additionally, it can regulate at a distance the cellular properties of adjacent germline cells**.**

The function of Dronc in ovarian somatic cells relies on its catalytic activity but is largely independent of the apoptosis programme

Most functions of caspases rely on their enzymatic activity, but some of the non-apoptotic roles require only protein-protein interactions[27, 28]. To determine whether *Dronc* mutant phenotypes were correlated with its enzymatic activity, we used a new conditional allele that contains after the FRT-rescue cassette a *Dronc* allele encoding a catalytically inactive protein[24]. This inactive version of Dronc contains two mutations, C318A and E352A, which compromise its enzymatic function and proteolytic activation[29, 30]. This mutant allele behaves as a null in homozygous conditions and is referred hereafter as *Dronc*-FL-CAEA ($Dronc^{KO\text{-}FRT\ Dronc\text{-}GFP\text{-}Apex\ FRT\text{-}Dronc\ FL\text{-}CAEA\text{-}Suntag\text{-}HA\text{-}Cherry}$)[24]. Upon excision of the wildtype rescue cassette, the expression of *Dronc*-FL-CAEA mutant protein recapitulated the loss of Castor expression and the cell proliferation defects in the 2b region of the germarium (Fig. 2g). Since these experiments indicated a requirement for the enzymatic activity of Dronc, we investigated the potential contribution to the Dronc phenotypes of its primary substrates in many cellular contexts, the effector caspases (drICE, DCP-1, Decay and Damm)[31]. To avoid a potential functional redundancy between these caspase members[32], we simultaneously targeted their expression by overexpressing

at the same time validated RNAi constructs against all of them[31]. These genetic manipulations produced weaker phenotypes than the *Dronc* loss-of-function (LOF), but still compromised Castor expression (Fig. 2g). Next, we analysed the role of the main upstream pro-apoptotic factors by targeting their expression via a micro RNA (UAS-RHG miRNA: *rpr*, *hid*, and *grim*)[33]. Strikingly, the concomitant elimination of *hid*, *reaper* and *grim* expression did not affect Castor levels (Fig. 2g). Collectively, these results indicate that *Dronc* functions in our cellular scenario demand its enzymatic activity and the subsequent activation of effector caspases, but are largely independent of the apoptotic programme.

Dronc activation promotes Hh-signalling in escort cells and follicular stem progenitors

Since Hh-signalling deficiency in escort and follicular stem cells generates phenotypes highly reminiscent of our *Dronc* mutant conditions[8, 9] (compare Fig. 2 with Supplementary Fig. 2a-c), we assessed the expression levels of standard read-outs of Hh-signalling in *Dronc* mutant cells. *Dronc* deficiency in follicular stem cells reduced the levels of the transcriptionally active form of Cubitus interruptus (Ci-155[34], Gli in mammals*;* compare Fig. 3a and 3b). Accordingly, the transcriptional activation of *ptc* was also compromised (compare Figure 3a with 3b; Supplementary Fig. 2d). The downregulation of both markers in *Dronc* mutant cells was a strong indication of Hh-signalling defects. To functionally confirm the crosstalk between caspases and Hh-signalling, we attempted to rescue the *Dronc* mutant phenotypes by overexpressing either a constitutively active form of Smo[15] (Fig. 3c, d) or Ci (Supplementary Fig. 2e, f). The individual overexpression of any of these Hh-components restored Castor expression and the proliferation defects of *Dronc* mutant cells (Fig. 3e). These data directly associated the *Dronc* LOF phenotypes in the germarium with Hh-signalling defects. Furthermore, they genetically placed *Dronc* upstream of *smo*.

Dronc regulates Hh-signalling through the fine-tuning of Ptc

Since our previous experiments placed the activation of Dronc upstream of *smo*, we investigated a potential genetic interaction between *Dronc* and *ptc*. A Gal4 P-element insertion in the regulatory region of *ptc* generated a weak LOF allele and a Gal4 line[35]. Unexpectedly, double heterozygous germaria *ptc*-Gal4:*Dronc*^{KO} (*ptc*-Gal4/+; *Dronc*^{KO} /+) phenotypically resembled the homozygous mutant condition for *Dronc;* Castor expression was downregulated (Fig. 4a-c) and Orb territory was expanded

(Fig. 4d-f). These phenotypes were also correlated with Hh-signalling defects, as indicated by Ci downregulation (Supplementary Fig. 2g). To validate this unanticipated interaction, we overexpressed a *Dronc*-RNAi construct under the regulation of the *ptc*-Gal4 driver (Supplementary Fig. 2h), and created double heterozygous flies harbouring a null allele of *ptc* (*ptc*^{S2}) and our *Dronc*^{KO} (*ptc*^{S2}/+; *Dronc*^{KO}/+, Supplementary Figure 2i). All of these genetic combinations showed comparable phenotypes. Furthermore, the observed phenotypes were dose-dependent and worsen by fully eliminating *Dronc* expression (*ptc*-Gal4/UAS-*flp*; *Dronc*^{KO}/ *Dronc*$^{FRT\text{-}Dronc\text{-}FRT\text{-}QF}$; Figure 4c, 4f-h). Collectively, these results suggested a clear, but initially counterintuitive, genetic interaction between *ptc* and *Dronc.* Since *ptc* is the receptor of Hh but acts a negative regulator of signalling, one would expect the upregulation of the pathway in *ptc* LOF conditions. Instead, the double insufficiency of *ptc* and *Dronc* severely compromised Hh-signalling.

To better understand the interaction between *Dronc* and *ptc*, we investigated the protein levels of the latter. Strikingly, although *ptc* was transcriptionally downregulated in *Dronc* mutant cells (Figure 3b), the protein levels were increased (Fig. 4i,j and Supplementary Fig. 3a). A detailed immunofluorescent analysis also revealed that Ptc positive particles were significantly enlarged in double heterozygous mutant germaria *ptc*-Gal4:*Dronc*^{KO} (Supplementary Fig. 3b). Confirming the association of *Dronc* phenotypes with Ptc aggregates, we largely rescued the Hh-signalling defects of *Dronc* mutant cells by preventing Ptc accumulation (Supplementary Fig. 3c-e). Recently, it has been described that Ptc can induce autophagy independently of its Hh-signalling regulatory role in mammalian cells and the *Drosophila* ovary[17, 36]. Therefore, we analysed whether the Ptc aggregates within *Dronc* mutant cells were competent to induce autophagy. To assess the autophagy flux in the germarium we used as a read-out the levels of Ref2P (the *Drosophila* ortholog of the mammalian p62). p62 is upregulated in cells with the autophagy process compromised, and downregulated upon autophagy activation[37]. As indicated by the downregulation of Ref2P, the autophagy flux was enhanced in *Dronc* mutant cells (Fig. 4k, 4l and Supplementary Fig. 3f). Collectively, these findings indicated that the non-apoptotic activation of Dronc modulates Ptc levels, and secondarily the activation of the Hh-pathway and the autophagy flux.

The caspase-mediated modulation of Hh-signalling and autophagy is evolutionarily conserved in human ovarian carcinoma cells

To evaluate the evolutionary conservation of our *Drosophila* findings, we used a human ovarian cell line with somatic origin (OVCAR-3). This cell line, like many others of similar origin, shows a basal hyperactivation of Hh-signalling[38]. We first downregulated the expression of *caspase-9* using specific siRNAs (Fig. 5a), and then monitored the activation of the Hh-pathway by Q-PCR. A previously validated set of primers [39] was used to estimate the transcriptional levels of the universal Hh-target gene *ptch1*. As observed in *Drosophila* cells, *caspase-9* deficiency compromised the transcriptional activation of *ptch1* and therefore we conclude that Hh-signaling is altered in *caspase-9* deficient cells (Fig. 5b). Next, we investigated the impact of caspase deficiency on the autophagy flux, using as marker p62[37]. The protein levels of p62 did not change in *caspase-9* mutant cells grown in standard cell culture conditions; however, they were consistently reduced in *capase-9*-deficient cells exposed to low concentrations of EtOH (Fig. 5c and 5d). EtOH has been shown to induce cellular stress (mainly reactive oxygen species) and autophagy through multiple molecular pathways in many cell types [40]. Confirming the specificity of the *caspase-9* effects on the autophagy, inhibition of this cellular process with bafilomycin[41] rescued the downregulation of p62 in *caspase-9* mutant cells exposed to EtOH (Fig. 5c and 5d). Collectively, these findings suggest that caspases can also modulate the levels of Hh-signalling and autophagy under moderate stress conditions in human ovarian cells with somatic origin.

DISCUSSION

Non-apoptotic activation of Dronc acts as a pro-survival factor in ovarian somatic stem cells

Our results show that the non-apoptotic activation of caspases modulates Hh-signalling and autophagy in ovarian somatic cells. Furthermore, these non-apoptotic caspase roles ensure the proper implementation of basic cellular functions such as cell proliferation, cell differentiation, and intercellular communication. These findings caution against the generic association of non-apoptotic patterns of caspase activation with the phenomenon of anastasis (pure recovery of caspase-activating cells from the “brink of death”)[42, 43]. Alternatively, they support the hypothesis that non-apoptotic caspase activation could be essential for regulating signalling events and cellular functions beyond apoptosis during development and adulthood [1-4].

Molecular basis of the caspase-dependent regulation of Hh-signalling and autophagy

At the molecular level, we show that sublethal levels of Dronc activation prevents the accumulation of Ptc receptor, and consequently alleviates its physiological inhibitory role on Hh-pathway (Fig. 5e). However, several factors suggest that Dronc is unlikely to directly cleave Ptc. First, there is no indication *in silico* that Ptc can be directly cleaved by Dronc. Second, the functional targets of Dronc in somatic cells appear to be the effector caspases (Fig. 2g). Third, the genetic interaction between *Dronc* and *ptc* is highly specific to the *Drosophila* germarium (e.g. both factors coexist in many other *Drosophila* tissues without any obvious signs of interaction). Therefore, although we provide the first mechanistic demonstration of the non-apoptotic interplay between caspases and Hh-signalling, unidentified molecular factors must couple their activities in ovarian somatic cells (Fig. 5e). Interestingly, it has been shown in mammalian cells that a set of ubiquitin ligases involved in the degradation of Ptc can also activate caspase-9 (*Dronc* mammalian homolog) and secondarily apoptosis in Hh-signalling deficient cells[44, 45]. However, it is unlikely that the equivalent *Drosophila* ubiquitin ligase (*smurf*) can explain our phenotypes since its expression and function are neither specific to the ovary or restricted to the Hh-pathway[46]. Nonetheless, our findings indicate that the crosstalk between caspases and Hh-signaling is more complex than anticipated, bidirectional and not specific to apoptosis.

Beyond modulating Hh-signalling and different cellular functions, Ptc aggregates in *Dronc* mutant cells can boost the autophagy levels (Fig. 4 and 5e). Although previous studies have associated *Dronc* with the regulation of autophagy [47, 48], our findings establish the first molecular link between this cellular process, Hh-pathway and *Dronc*. In parallel, they also confirm the novel regulatory role of Ptc in the autophagy process [17]. Nevertheless, *Dronc* mutant phenotypes can be largely rescued by reactivating the Hh-pathway, and therefore the potential contribution of the autophagy to the *Dronc* phenotypes must be secondary. Interestingly, like in *Dronc* mutant cells, *caspase-9* deficiency appears to enhance the autophagy in human ovarian cells under moderate stress and induced-autophagy conditions (Fig. 5c and 5d). Together, these results suggest that caspases are part of the evolutionary conserved genetic network regulating Hh-pathway and autophagy in ovarian somatic cells.

Cellular, physiological and evolutionary implications of non-apoptotic caspase activation in ovarian somatic cells

Our findings have shown the stereotyped presence of non-apoptotic caspase activation in somatic cells of the *Drosophila* ovary under physiological or moderate stress conditions. Indeed, this caspase activation appears to promote cell proliferation and differentiation in this context. Consequently, we propose that caspases are at the forefront of the cell survival mechanisms against cellular stress in ovarian somatic cells. Additionally, sustained caspase activation due to persistent signalling defects and/or environmental stress leads to apoptosis[49]. This dual role of caspases, coupled to different signalling pathways, could be an effective mechanism of signalling compensation and cellular selection in multiple cellular scenarios[50]. Future investigations are needed to unravel whether caspase activation to only sublethal thresholds is ensured via either specialised molecular mechanisms in specific subcellular localisations[51], the strength of the activating cues, or a combination of both factors.

From a physiological perspective, it is well-described that Hh downregulation triggered by environmental stress restricts egg laying and promotes autophagy in *Drosophila*[52-54]. Similarly, Hh deregulation and/or exacerbated autophagy can compromise follicular development in mammalian systems[55, 56]. Our work suggests that sublethal caspase activation influences Hh-signalling and autophagy, and therefore it is also part of the complex adaptive system that ensures timely egg maturation.

Considering the described non-apoptotic roles of ancient members of the caspase family (metacaspases)[4, 57, 58], our data may also have evolutionary implications. Since *Dronc* initially plays a pro-survival role in somatic cells, our results support the hypothesis that the primary role of caspases could be for sustaining basic cellular processes, and only inadvertent/persistent activation would lead to cell death[57]. In this view, these pro-apoptotic enzymes would primarily act as pro-survival factors, thus inverting the widely held view of their most primitive function. A greater understanding of the non-apoptotic roles of caspases is needed to test this hypothesis.

Pathological and therapeutic consequences of caspase malfunction in ovarian somatic cells

Caspase activation can not only facilitate follicular development (our results), but also degeneration and follicular atresia in mammalian systems[59]. Therefore, caspase deregulation could compromise ovarian function through different mechanisms. On

one hand, caspase deficiency can alter the progression of follicular development by compromising the activation of key developmental signalling pathways such as Hh. On the other hand, it can prevent the natural degeneration of redundant follicles[59]. The combination of both effects can lead to ovarian failure, whilst creating tumour prone conditions. Furthermore, since the combined upregulation of Hh-signalling and autophagy is key to explaining the drug resistance of ovarian tumours[60-62], caspase malfunctions acting upstream of these factors could compromise the success of therapeutic interventions. Paradoxically, our results also indicate that the therapeutic re-activation of caspases in the ovary also requires a careful calibration since sublethal caspase activation could promote the clonal expansion of somatic malignant cells. Collectively, these considerations illustrate some of the complexities of transferring caspase-modulating molecules into the clinic[63].

MATERIAL AND METHODS

Fly Strains and fly husbandry details

All fly strains used are described at www.flybase.bio.indiana.edu unless otherwise indicated. After 24h of egg laying at 25°C, experimental specimens were raised at 18°C, thus enabling the repression of Gal4 activity through a $Gal80^{ts}$. This prevents potential lethality in most of our experimental conditions during larval and pupal stages. After hatching, adults were then transferred from 18°C to 29°C until the dissection time. At 29°C the repression of $Gal80^{ts}$ disappears, and therefore gene expression via Gal4 is elicited within specific cell subpopulations of the germarium.

Genotypes

Full description of experimental genotypes appearing in each figure.

Fig. 1

1b. *Actin DBS-S-QF, UAS-mCD8-GFP, QUAS-tomato-HA/+;; QUAS-Gal4/+*

1c and **1d**. *Actin DBS-S-QF, UAS-mCD8-GFP, QUAS-tomato-HA/+; QUAS-FLP (BL30126)/+; Actin5C FRT-stop-FRT lacZ-nls/+ (BL6355)*

1f. *w;; $Dronc^{KO\text{-}Gal4}$ / UAS-Histone-RFP (BL56555)*

1g. *UAS-FLP (BL4539) /+; $Dronc^{KO\text{-}Gal4}$ / Actin5C FRT-stop-FRT lacZ-nls (BL6355)*

Fig. 2

2a and **2c**, left panel. *109-30Gal4 (BL7023)/+; $Dronc^{KO}$ $Tub\text{-}G80^{ts}$ (BL7019) / +.* The bars in 2b and 2d referring to this experiment are named as CTRL.

2a and **2c**, right panel. *109-30Gal4 (BL7023)/ QUAS-CD8-GFP (BL 30002); Dronc^{KO} Tub-G80^{ts} (BL7019) / UAS-Flp (BL8209) Dronc$^{KO\text{-}FRT\text{-}Dronc\text{-}GFP\text{-}APEX\text{-}FRT\text{-}QF}$*. The bars in 2b and 2d referring to this experiment are named as *Dronc* -/-.

2e and **2f**, left panel. *spitz-Gal4 (NP0261)/+; Dronc^{KO} Tub-G80^{ts} (BL7019)* / +. The bars in 2b and 2d referring to this experiment are named as CTRL.

2e and **2f**, right panel. *spitz-Gal4 (NP0261)/ QUAS-CD8-GFP (BL 30002); Dronc^{KO} Tub-G80^{ts} (BL7019) / UAS-Flp (BL8209) Dronc$^{KO\text{-}FRT\text{-}Dronc\text{-}GFP\text{-}APEX\text{-}FRT\text{-}QF}$*. The bars in 2b and 2d referring to this experiment are named as *Dronc* -/-.

2g. First bar, *109-30Gal4 (BL7023)/ QUAS-CD8-GFP (BL 30002); Dronc^{KO} Tub-G80^{ts} (BL7019) / UAS-Flp (BL8209) Dronc$^{KO\text{-}FRT\ Dronc\text{-}GFP\text{-}Apex\ FRT\text{-}Suntag\text{-}HA\text{-}Cherry}$* . Second bar, *109-30Gal4 (BL7023)/ QUAS-CD8-GFP (BL 30002); Dronc^{KO} Tub-G80^{ts} (BL7019) / UAS-Flp (BL8209) Dronc$^{KO\text{-}FRT\ Dronc\text{-}GFP\text{-}Apex\ FRT\text{-}Dronc\ FL\text{-}CAEA\text{-}Suntag\text{-}HA\text{-}Cherry}$* . Third bar, *109-30Gal4 (BL7023)/UAS-DriceRNAi UAS-DecayRNAi (a gift from Pascal Meier); UAS-DammRNAi, UAS-Dcp1RNAi (a gift from Pascal Meier).* Fourth bar; *109-30Gal4 (BL7023)/ UAS-RHG.miRNA (a gift from Iswar Hariharan)*

Fig. 3

3a. *109-30Gal4 (BL7023)/ ptc-GFP* ^{CB02030} (a gift from Isabel Guerrero)

3b. *109-30Gal4 (BL7023)/ ptc-GFP* ^{CB02030} (a gift from Isabel Guerrero)*; Dronc^{KO} Tub-G80^{ts} (BL7019) / UAS-Flp (BL8209) Dronc$^{KO\text{-}FRT\text{-}Dronc\text{-}GFP\text{-}APEX\text{-}FRT\text{-}QF}$*

3c. *109-30Gal4 (BL7023)/UAS-smo^{Act} (BL44621); Dronc^{KO} Tub-G80^{ts} (BL7019)* / +

3d. *109-30Gal4 (BL7023)/UAS-smo^{Act} (BL44621); Dronc^{KO} Tub-G80^{ts} (BL7019) / UAS-Flp (BL8209) Dronc$^{KO\text{-}FRT\text{-}Dronc\text{-}GFP\text{-}APEX\text{-}FRT\text{-}QF}$*

3e. First bar (*Dronc* -/-), *109-30Gal4 (BL7023)/+; Dronc^{KO} Tub-G80^{ts} (BL7019) / UAS-Flp (BL8209) Dronc$^{KO\text{-}FRT\text{-}Dronc\text{-}GFP\text{-}APEX\text{-}FRT\text{-}QF}$*. Second bar (CTRL1), *109-30Gal4 (BL7023)/UAS-Ci (BL32571); Dronc^{KO} Tub-G80^{ts} (BL7019)/+.* Third bar (Dronc -/-, UAS-Ci); *109-30Gal4 (BL7023)/UAS-Ci (BL32571); Dronc^{KO} Tub-G80^{ts} (BL7019) / UAS-Flp (BL8209) Dronc$^{KO\text{-}FRT\text{-}Dronc\text{-}GFP\text{-}APEX\text{-}FRT\text{-}QF}$*. Fourth bar (CTRL2); *109-30Gal4 (BL7023)/UAS-smo^{Act} (BL44621); Dronc^{KO} Tub-G80^{ts} (BL7019)* / +. Fifth bar (Dronc -/-, UAS-*smo*^{Act}); *109-30Gal4 (BL7023)/UAS-smo^{Act} (BL44621); Dronc^{KO} Tub-G80^{ts} (BL7019) / UAS-Flp (BL8209) Dronc$^{KO\text{-}FRT\text{-}Dronc\text{-}GFP\text{-}APEX\text{-}FRT\text{-}QF}$*. The first and third bars are named in graph as CTRL, while the second and the fourth as *Dronc* -/-.

Fig. 4

4a and **4d.** *ptc-Gal4$^{559.1}$ (BL2017)/+*

4b and **4e**. *ptc-Gal4$^{559.1}$ (BL2017)/+; Dronc+/-*

4c and **4f.** First bar, *ptc-Gal4$^{559.1}$ (BL2017)/+.* Second bar, *ptc-Gal4$^{559.1}$ (BL2017)/+; Dronc+/-.* Third bar, *ptc-Gal4$^{559.1}$ (BL2017)/ QUAS-CD8-GFP (BL 30002); Dronc^{KO} Tub-G80^{ts} (BL7019) / UAS-Flp (BL8209) Dronc$^{KO\text{-}FRT\text{-}Dronc\text{-}GFP\text{-}APEX\text{-}FRT\text{-}QF}$*

4g and **4h**. *ptc-Gal4$^{559.1}$ (BL2017)/ QUAS-CD8-GFP (BL 30002); Dronc^{KO} Tub-G80^{ts} (BL7019) / UAS-Flp (BL8209) Dronc$^{KO\text{-}FRT\text{-}Dronc\text{-}GFP\text{-}APEX\text{-}FRT\text{-}QF}$*

4i-l. First bar, *Dronc^{KO}/+.* Second bar, *ptc-Gal4$^{559.1}$ (BL2017)/ +.* Third bar, *ptc-Gal4$^{559.1}$ (BL2017)/ + ; Dronc^{KO}/+*

Immunohistochemistry

Adult *Drosophila* ovaries were dissected on ice-cold PBS. Immunostainings and washes were performed according to standard protocols (fixing in PBS 4% paraformaldehyde, washing in PBT 0.3% (0.3% Triton X-100 in PBS). Primary antibodies used in our experiments were: anti-Castor (1:2000; a gift from Alex Gould); rabbit anti-HA (1:1000; Cell Signaling C29F4); mouse anti-betaGal (1:500; Promega Z378B); chicken Anti-βGal (1:200, Abcam AB9361); Anti-FasIII (1:75, Hybridoma Bank 7G10); Anti-Orb (1:75, Hybridoma Bank 4H8), Anti-Ci-155-full length (1:50, Hybridoma Bank 2A1); Anti-Ptc (1:50, Hybridoma Bank Apa1); Anti-Ref2P (1:300, abcam 178440). Conjugated secondary antibodies (Molecular Probes) were diluted in 0.3% PBT and used in a final concentration (1:200): conjugated donkey anti-rabbit Alexa-Fluor- 488 (A21206) or 555 (A31572) or 647 (A31573), conjugated donkey anti-mouse Alexa-Fluor-488 (A21202) or 555 (A31570) or 647 (A31571), conjugated goat anti-rat Life Technologies (Paisley, UK) Alexa-Fluor- 488 (A21247) or 555 (A21434). DAPI was added to the solution with the secondary antibodies for labelling the nuclei (1:1000; Thermo Scientific 62248). Following incubation in secondary antibodies, samples were washed several times during 60 minutes in PBT. Finally, they were mounted on Poly-Prep Slides (P0425-72EA, Sigma) in Aqua-Poly/Mount (Polysciences, Inc (18606)).

TUNEL staining

Like in the immunochemistry, follicles from adult *Drosophila* females were dissected in ice-cold PBS and fixed in PBS containing 4% formaldehyde for 20'. After fixation, the samples were washed 3 times for 15' with PBS and subsequently permeabilised with PBS containing 0,3% triton and 0,1% sodium citrate for 8' on ice. 3 PBS washes for 20' with were performed also after permeabilisation. The *in situ* detection of fragmented genomic DNA was performed according to the DeadEnd colorimetric

TUNEL (Terminal transferase-mediated dUTP nick-end labeling) system (Promega). Briefly, samples were first equilibrated at room temperature in equilibration buffer (5-10') and then incubated with TdT reaction mix for 1 hour at 37°C in a humidified chamber to obtain the 3'-end labelling of fragmented DNA. The reaction was terminated with 3 washes for 15' in PBS. If necessary, the TUNEL protocol was followed by standard immunofluorescent staining. The detection of TUNEL-positive cells was achieved by an incubation of 45' with streptavidin-fluorophore conjugated dyes.

Imaging of fixed and live samples

Drosophila ovarioles were imaged using the Olympus Fluoview FV1200 and associated software. Z-stacks were taken with a 40X objective at intervals along the apical-basal axis that ensured adequate resolution along Z-axis (step size 0.5-1.5-µm). The same confocal settings were used during the image acquisition process of experimental and control samples. Acquired images were processed using ImageJ 1.52n software[64] and Adobe Photoshop CC in order to complete the figure preparation.

Image quantification

All of the images used in this study were randomised and blindly scored during the quantification process. Images for quantification purposes were processed with ImageJ 1.52n. To estimate the percentage of germaria showing Castor expression defects (Fig 2b, 2g, 3e, 4c and Suppl Fig 2c, 3e), we first projected at least 8 focal planes (maximum projection plug-in included in ImageJ) containing the follicular cells of region 2b forming the arch-like structure around the germline. The germaria were considered mutant for Castor if showing more than two follicular cells negative for this gene in the 2b region.

In all other quantifications, all of the focal planes of each ovariole were first merged using the maximum projection plug-in included in ImageJ. The relative area of the germaria occupied by Orb-expressing cells (Fig 2d, 4f) was estimated as follows. First, we delimited with the freehand selection tool of ImageJ the area occupied by Orb-expressing cells and subsequently, we used the corresponding plugin of the software to estimate the area. Following the same workflow, we next estimate the total area of the germarium. The value of area of Orb-expressing cells was finally divided by the total area of the germaria.

After applying the thresholding and "Analyse Particles" plug-in from ImageJ, we quantified the number and size of Ptc and Ref2P-positive particles in the regions 1, 2a and 2b of the germarium (Fig 4i, 4k, Supp Fig 3b).

The "mean grey value" of the GFP channel in regions 1, 2a and 2b of the germaria was used to estimate the intensity of GFP signal derived from the *ptc*-GFP transgene (Supp Fig 2d).

Western Blot

Adult *Drosophila* ovaries were dissected in ice-cold PBS and snap-frozen in liquid nitrogen. Subsequently, they were homogenised in NP40 buffer [150 mM NaCl, 50 mM Tris-HCl pH 7.5, 5% glycerol, 1% IGEPAL CA-630]. Cells were harvested using trypsin/EDTA and centrifuged at 300g for 5'. Pellets were washed in PBS and then treated with RIPA lysis buffer 1x [150 mM NaCl, 50 mM Tris-HCl pH 7.5, 0.1 mM EGTA, 0,5 mM EDTA, 1% Triton X-100]. Halt Protease and Phosphatase Inhibitor Cocktail (Thermo Scientific Pierce) and Benzonase (BaseMuncher, Expedeon) were added according to the manufacturer's instructions. Protein content was determined using Bradford reagent (Bio-Rad). Extracts were mixed with NuPAGE LDS Sample Buffer and separated by SDS-PAGE. For performing the SDS-PAGE electrophoresis, lysates were loaded and run in NuPAGE Bis-Tris Gels in NuPAGE MOPS SDS Running Buffer (Thermofisher Scientific). Protein blot transfers were performed using Trans-Blot Turbo Transfer System (Biorad). Nitrocellulose blots were incubated at room temperature for 30' in blocking buffer [Tris-buffered saline with 0.1% Tween containing 5% non-fat dried milk] and then incubated overnight at 4°C in the same blocking solution with the corresponding antibodies. After washing three times for 15' each with Tris-buffered saline containing 0.1% Tween, the blots were incubated with horseradish peroxidase-conjugated (HRP) IgG, followed by washing. Immunoreactive bands were detected using the SuperSignal West Pico PLUS Chemiluminescent Substrate (Thermofisher Scientific). Developed CL-XPosure films (Thermofisher Scientific) were scanned using a flat-bed scanner and the density of the bands was measured using Gel Analyzer plugin in ImageJ software. Primary antibodies used: Anti-Ptc (1:500, Hybridoma Bank Apa1); Anti-Ref2P (1:500, abcam 178440); Anti-Actin (1:500, Hybridoma Bank JLA20s); Anti-Ci-155-full length (1:500, Hybridoma Bank 2A1); Anti-Caspase-9 (C9) (1:1000, Cell Signalling 9508); Anti-β-Actin−Peroxidase (1:20000, Sigma A3854), Anti SQSTM1 / P62 antibody (1:5000, GeneTex GTX111393).

Cell culture mammalian cells

OVCAR-3 cells were maintained in RPMI (Sigma, R8758), supplemented with 10% FBS (Life Technologies, 10500064) and grown at 37°C in a humidified atmosphere with 5% CO_2. For the experiment shown in Figure 5c and 5d, we replaced the media with fresh media containing either EtOH (0.2%) or EtOH (0.2%) + the inhibitor of autophagy bafilomycin A1 (400nM, Merck Chemicals). Cells were grown in these two different cell culture media during the last 4 hours previous the sample processing.

RNA interference

Small interfering RNA (siRNA) specific for Caspase-9 (ON-TARGETplus SMART pool human L-003309-00-0005, 842), PTCH1 (ON-TARGETplus Human PTCH1, L-003924-00-0005, 5727) and non-targeting controls (ON-TARGET plus Non-targeting Pool, D-001810-10-05) were purchased from Dharmacon Inc. (UK). Cells were plated and transfected the day after with Oligofectamine™ Transfection Reagent (Thermofisher 12252) in the presence of siRNAs according to the manufacturer's instructions. Cells were kept in the transfection mix before processing for western blot or Q-PCR at the specified time points (24h and 72h).

Gene expression analyses by Q-PCR.

RNA extraction was performed using the Qiagen RNeasy Plus kit (74034). cDNAs were synthesised with Maxima First Strand cDNA synthesis kit (Molecular Biology, Thermofisher, K1642) Q-PCR were performed using QuantiNova SYBR Green PCR Kit (Qiagen, 208054). Detection was performed using Rotor-Gene Q Real-time PCR cycler (Qiagen).

Data was analysed using the Pfaffl method, based on ΔΔ−Ct and normalised to actin as the housekeeping gene.

Gene expression was estimated with the following primers:

Patched1: Forward CCACGACAAAGCCGACTACAT; Reverse GCTGCAGATGGTCCTTACTTTTTC

B-actin: Forward CCTGGCACCCAGCACAAT; Reverse GGGCCGGACTCGTCATAC.

FIGURE LEGENDS:

Fig. 1 Non-apoptotic caspase activation in the somatic cells of the *Drosophila* germarium.

a, Schematic drawing of the *Drosophila* germarium. Somatic cells relevant for this study (escort, follicular stem and follicular) are depicted in different colours; germline

cells are in white. **b**, Representative confocal image of past (green channel, arrows) and present (red channel) caspase activation in somatic cells using the DBS-S-QF sensor; TUNEL staining indicates apoptosis (grey channel). **c**, Representative confocal image of escort and follicular somatic cells permanently labelled with DBS-S-QF sensor (green channel, arrows); the arrowhead indicates the presence of apoptotic germline cells (red channel, TUNEL staining). Notice the lack of TUNEL signal in DBS-S-QF positive cells in c. **d**, Graph bar indicating the percentage of ovarioles permanently labelled with DBS-S-QF sensor at 7 and 14 days; flies were raised at 18°C until eclosion, then shifted to 29°C until the dissection time. **e**, Graphical representation of the *Dronc*$^{KO\text{-}Gal4}$ expression pattern in the germarium; cells transcribing *Dronc* are coloured in red. **f**, Representative example of somatic cells in the germarium expressing Histone-RFP (red channel) under the regulation of *Dronc*$^{KO\text{-}Gal4}$ at 29 ^{o}C; the follicular maker Castor is shown in green. **g**, Representative example of a cell lineage-tracing experiment conducted using *Dronc*$^{KO\text{-}Gal4}$; notice the presence of *Dronc* expressing cells in the escort cell territory and the region 2b of the germarium (green channel shows anti-Bgal staining). Follicular somatic cells are labelled with anti-FasIII (red channel in g). Dapi staining labels the nuclei (blue channel) in all the confocal images. Please see full genotype description in the MM section. Scale bars represents 10 µm.

Fig. 2 Phenotype characterisation of caspase loss-of-function in the *Drosophila* germarium.

a, Confocal image comparing the expression of the follicular cell marker Castor (red and grey channels) in either heterozygous (left side of the white dotted line) or homozygous *Dronc* mutant follicular cells (right side) generated using 109-30-Gal4; notice the downregulation of Castor in the mutant condition (arrow). GFP signal labels *Dronc*-transcribing cells (green channel, QUAS-CD8-GFP) after preferentially excising the *Dronc* FRT-rescue-cassette in the follicular stem cells and their progeny (region 2b of the germarium) using the 109-30-Gal4 driver. Dapi labels the nuclei in a, c, e, and f, respectively. **b**, Cumulative percentage of Castor-deficient germaria in either heterozygous or homozygous *Dronc* mutant cells using different Gal4 drivers (109-30, *spitz*, and c587); the n number for each column in order of appearance n=16, n=17, n=20, n=15, n=34, n=19. **c**, Orb expression (red and grey channels) in a heterozygous (left side) or homozygous *Dronc* mutant background (right side); *Dronc* expression was targeted in the follicular stem cells and their progeny (region 2b of the germarium) using 109-30-Gal4. **d,** Relative area occupied by Orb-expressing

cells; Gal4 drivers used were 109-30, *spitz,* and c587; n=12, n=20, n=17, n=17, n=18, n=6; statistical significance was established by using an ordinary Unpaired T-test (* p≤0.05, ** p≤0.01, ***p≤0.001). **e** and **f**, Castor and Orb expression in a heterozygous (left side) or homozygous *Dronc* mutant escort cells (right side) (red and grey channels in e and f, respectively) generated using *spitz*-Gal4. **g**, Percentage of Castor-deficient germaria after compromising the expression of Dronc (first bar, n=11, Dronc suntag-HA-Cherry/-), the activation of Dronc (second bar, n=15, Dronc-FL-CAEA /-), the expression of all of the effector caspases (third bar, n=16, UAS-RNAi) and the expression of proapoptotic factors (fourth bar, n=9, microRNA against the major pro-apoptotic factors *hid*, *grim* and *reaper*). Full genotype description in the MM section. Scale bars represents 10 μm.

Fig. 3 The loss-of function of *Dronc* causes Hh-signalling defects.

a and **b**, Representative confocal image showing the expression of Ci-155 (blue and grey channels), *ptc*-GFP (*ptc*-GFP is a *bona-fide* transcriptional read out of Hh-pathway[65]; green and grey channels) and Castor (red and grey channels) in either a control (a) or a *Dronc* mutant germarium (b); notice the downregulation of *Ci* and *ptc*-GFP expression. **c**, Castor expression (red and grey channels) in follicular cells heterozygous for *Dronc* expressing a constitutively active form of *smo* under the regulation of 109-30-Gal4 driver. **d**, Castor expression (red and grey channels) in follicular cells homozygous for *Dronc* expressing a constitutively active form of *smo* under the regulation of 109-30-Gal4 driver; notice that castor is not downregulated (compare with Fig.2). Dapi staining labels the nuclei in c and d. **e**, Cumulative percentage of Castor-deficient germaria after expressing Ci or Smo-activated under the regulation of 109-30-Gal4 in either heterozygous or homozygous *Dronc* follicular mutant cells; the n number for each column in order of appearance n=21, n=8, n=24, n=11, n=8. Full genotype description in the MM section. Scale bars represents 10 μm.

Fig. 4 *Dronc* modulates Hh-signalling and autophagy through the fine regulation of Ptc protein levels.

a and **b**. Castor expression (red and grey channels) in either a *ptc* heterozygous germarium (a) or double heterozygous *ptc-Dronc* (b); notice the downregulation of Castor in b. Dapi staining (blue channel) labels the nuclei in all the confocal images of the figure. **c**, Cumulative percentage of Castor-deficient germaria in the genetic conditions indicated in the graph; the n number for each column in order of

appearance n=20, n=25, n=20. **d** and **e**, Orb expression (red and grey channels) in either a *ptc* heterozygous germarium (d) or double heterozygous *ptc-Dronc* (e). **f**, Relative area occupied by Orb-expressing cells in the genetic conditions indicated in the graph, an ordinary one-way ANOVA Tukey's multiple comparisons test was used to establish the statistical significance (*** p≤0.001, ****p≤0.0001). **g** and **h**, Castor (red and grey channels in g) and Orb (red and grey channels in h) expression in *ptc* heterozygous-*Dronc* fully mutant germaria; notice the downregulation of Castor (g) and the accumulation of Orb-expressing cells (h). *Dronc*-transcribing cells are labelled with GFP (green channel, QUAS-CD8-GFP) upon excision in the escort and the follicular cells of the *Dronc* FRT-rescue-cassette using the *ptc*-Gal4 driver. **i**, Relative number of Ptc positive particles per germaria; notice the increased number of Ptc particles in double heterozygous germaria (*ptc*-Gal4/+;*Dronc* +/-) , an ordinary one-way ANOVA Tukey's multiple comparisons test was used to establish the statistical significance (*** p≤0.001). **j**, Western blot showing Ptc (upper lane) and Actin (bottom lane, loading control) in different genetic mutant backgrounds; notice the Ptc accumulation in double heterozygous germaria (*ptc*-Gal4/+;*Dronc* +/-). **k**, Relative number of the Ref2P positive particles per germaria; notice the reduction in the number of Ref2P particles in double heterozygous germaria (*ptc*-Gal4/+;*Dronc* +/-) compared to the (*ptc*-Gal4/+) control; an ordinary one-way ANOVA Tukey's multiple comparisons test was used to establish the statistical significance (** p≤0.01, ****p≤0.0001). **l**, Western blot showing Ref2P (upper lane) and Actin (bottom lane) in different genetic mutant backgrounds; notice the Ref2P reduction in double heterozygous germaria (*ptc*-Gal4/+;*Dronc* +/-) compared to the (*ptc*-Gal4/+) control. Full genotype description in the MM section. Scale bars represents 10 μm.

Fig. 5 The non-apoptotic caspase effects in Hh-signalling and autophagy are evolutionarily conserved in ovarian somatic cells with human origin.

a, Western blot showing caspase-9 expression (upper lane) and Actin (bottom lane, loading control) in either control or Caspase-9 mutant OVCAR-3 cells (24h and 72h post-transfection of an shRNA against Caspase-9; notice the strong downregulation of Caspase-9 at 72h. **b**, mRNA levels of *ptc* measured by Q-PCR in either control or Caspase-9 mutant OVCAR-3 cells; notice the strong downregulation of *ptc* expression in the Caspase-9 mutant cells at 72h; an ordinary Mann Whitney unpaired T-test was used to establish the statistical significance (** p≤0.01). **c**, Western blot showing the expression levels of the autophagy marker p62 (upper lane), Caspase-9 (middle lane) and Actin (bottom lane, loading control) in either

scrambled or caspase-9 mutant OVCAR-3 cells; the protein levels of the different read outs were measured at 72h after siRNA treatment in cells grown during the last 4 h before sample processing in our standard cell culture conditions, in cell culture media containing EtOH (0.2%), and in cell culture media containing EtOH (0.2%) + bafilomycin A1 (400nM). **d**, Quantification of p62 protein levels in the experimental conditions described in d; notice the dowregulation of p62 in EtOH treated cells deficient in Caspase-9 (one sample T Wilcoxon test was used to calculate statistical significance, * $p \leq 0.05$, $n \geq 3$. **e**, Model summarising the non-apoptotic effects of caspases in ovarian somatic cells with human origin. Green colour, big font and plus symbol (+) indicate activation, while red colour, small font and negative symbol (-) reflect downregulation. The cellular consequences of caspase activation/deficiency are indicated as Cellular Effects.

REFERENCES

1. Aram, L., Yacobi-Sharon, K. & Arama, E. CDPs: caspase-dependent non-lethal cellular processes. *Cell Death Differ* **24**, 1307-1310 (2017).
2. Baena-Lopez, L.A. All about the caspase-dependent functions without cell death. *Semin Cell Dev Biol* (2018).
3. Burgon, P.G. & Megeney, L.A. Caspase signaling, a conserved inductive cue for metazoan cell differentiation. *Semin Cell Dev Biol* (2017).
4. Bell, R.A.V. & Megeney, L.A. Evolution of caspase-mediated cell death and differentiation: twins separated at birth. *Cell Death Differ* **24**, 1359-1368 (2017).
5. Kirilly, D. & Xie, T. The Drosophila ovary: an active stem cell community. *Cell Res* **17**, 15-25 (2007).
6. Losick, V.P., Morris, L.X., Fox, D.T. & Spradling, A. Drosophila stem cell niches: a decade of discovery suggests a unified view of stem cell regulation. *Dev Cell* **21**, 159-171 (2011).
7. Tang, H.L., Tang, H.M., Fung, M.C. & Hardwick, J.M. In vivo CaspaseTracker biosensor system for detecting anastasis and non-apoptotic caspase activity. *Sci Rep* **5**, 9015 (2015).
8. Huang, J. & Kalderon, D. Coupling of Hedgehog and Hippo pathways promotes stem cell maintenance by stimulating proliferation. *J Cell Biol* **205**, 325-338 (2014).
9. Huang, J., Reilein, A. & Kalderon, D. Yorkie and Hedgehog independently restrict BMP production in escort cells to permit germline differentiation in the Drosophila ovary. *Development* **144**, 2584-2594 (2017).
10. Vied, C. & Kalderon, D. Hedgehog-stimulated stem cells depend on non-canonical activity of the Notch co-activator Mastermind. *Development* **136**, 2177-2186 (2009).
11. Zhang, Y. & Kalderon, D. Hedgehog acts as a somatic stem cell factor in the Drosophila ovary. *Nature* **410**, 599-604 (2001).
12. Rojas-Rios, P., Guerrero, I. & Gonzalez-Reyes, A. Cytoneme-mediated delivery of hedgehog regulates the expression of bone morphogenetic

proteins to maintain germline stem cells in Drosophila. *PLoS Biol* **10**, e1001298 (2012).

13. Sahai-Hernandez, P. & Nystul, T.G. A dynamic population of stromal cells contributes to the follicle stem cell niche in the Drosophila ovary. *Development* **140**, 4490-4498 (2013).
14. Chang, Y.C., Jang, A.C., Lin, C.H. & Montell, D.J. Castor is required for Hedgehog-dependent cell-fate specification and follicle stem cell maintenance in Drosophila oogenesis. *Proc Natl Acad Sci U S A* **110**, E1734-1742 (2013).
15. Briscoe, J. & Therond, P.P. The mechanisms of Hedgehog signalling and its roles in development and disease. *Nat Rev Mol Cell Biol* **14**, 416-429 (2013).
16. Dai, W., Peterson, A., Kenney, T., Burrous, H. & Montell, D.J. Quantitative microscopy of the Drosophila ovary shows multiple niche signals specify progenitor cell fate. *Nat Commun* **8**, 1244 (2017).
17. Singh, T., Lee, E.H., Hartman, T.R., Ruiz-Whalen, D.M. & O'Reilly, A.M. Opposing Action of Hedgehog and Insulin Signaling Balances Proliferation and Autophagy to Determine Follicle Stem Cell Lifespan. *Dev Cell* **46**, 720-734 e726 (2018).
18. Rosales-Nieves, A.E. & Gonzalez-Reyes, A. Genetics and mechanisms of ovarian cancer: parallels between Drosophila and humans. *Semin Cell Dev Biol* **28**, 104-109 (2014).
19. Szkandera, J., Kiesslich, T., Haybaeck, J., Gerger, A. & Pichler, M. Hedgehog signaling pathway in ovarian cancer. *Int J Mol Sci* **14**, 1179-1196 (2013).
20. Zeng, C., Chen, T., Zhang, Y. & Chen, Q. Hedgehog signaling pathway regulates ovarian cancer invasion and migration via adhesion molecule CD24. *J Cancer* **8**, 786-792 (2017).
21. Ray, A., Meng, E., Reed, E., Shevde, L.A. & Rocconi, R.P. Hedgehog signaling pathway regulates the growth of ovarian cancer spheroid forming cells. *Int J Oncol* **39**, 797-804 (2011).
22. Li, H., Li, J. & Feng, L. Hedgehog signaling pathway as a therapeutic target for ovarian cancer. *Cancer Epidemiol* **40**, 152-157 (2016).
23. Baena-Lopez, L.A. *et al.* Apical caspase reporters uncover unknown stages of apoptosis and enable ready visualization of undead cells. (2018).
24. Arthurton, L., Nahotko, D., Alonso, J. & Baena-Lopez, L.A. Non-apoptotic caspase-dependent regulation of enteroblast quiescence in Drosophila. *bioRxiv* (2019).
25. Baena-Lopez, L.A., Alexandre, C., Mitchell, A., Pasakarnis, L. & Vincent, J.P. Accelerated homologous recombination and subsequent genome modification in Drosophila. *Development* **140**, 4818-4825 (2013).
26. Jin, Z., Flynt, A.S. & Lai, E.C. Drosophila piwi mutants exhibit germline stem cell tumors that are sustained by elevated Dpp signaling. *Curr Biol* **23**, 1442-1448 (2013).
27. Napoletano, F. *et al.* p53-dependent programmed necrosis controls germ cell homeostasis during spermatogenesis. *PLoS Genet* **13**, e1007024 (2017).
28. Ouyang, Y. *et al.* Dronc caspase exerts a non-apoptotic function to restrain phospho-Numb-induced ectopic neuroblast formation in Drosophila. *Development* **138**, 2185-2196 (2011).

29. Muro, I., Monser, K. & Clem, R.J. Mechanism of Dronc activation in Drosophila cells. *J Cell Sci* **117**, 5035-5041 (2004).
30. Chai, J. *et al.* Molecular mechanism of Reaper-Grim-Hid-mediated suppression of DIAP1-dependent Dronc ubiquitination. *Nat Struct Biol* **10**, 892-898 (2003).
31. Leulier, F. *et al.* Systematic in vivo RNAi analysis of putative components of the Drosophila cell death machinery. *Cell Death Differ* **13**, 1663-1674 (2006).
32. Xu, D. *et al.* The effector caspases drICE and dcp-1 have partially overlapping functions in the apoptotic pathway in Drosophila. *Cell Death Differ* **13**, 1697-1706 (2006).
33. Siegrist, S.E., Haque, N.S., Chen, C.H., Hay, B.A. & Hariharan, I.K. Inactivation of both Foxo and reaper promotes long-term adult neurogenesis in Drosophila. *Curr Biol* **20**, 643-648 (2010).
34. Motzny, C.K. & Holmgren, R. The Drosophila cubitus interruptus protein and its role in the wingless and hedgehog signal transduction pathways. *Mech Dev* **52**, 137-150 (1995).
35. Shyamala, B.V. & Bhat, K.M. A positive role for patched-smoothened signaling in promoting cell proliferation during normal head development in Drosophila. *Development* **129**, 1839-1847 (2002).
36. Jimenez-Sanchez, M. *et al.* The Hedgehog signalling pathway regulates autophagy. *Nat Commun* **3**, 1200 (2012).
37. Bjorkoy, G. *et al.* Monitoring autophagic degradation of p62/SQSTM1. *Methods Enzymol* **452**, 181-197 (2009).
38. Bhattacharya, R. *et al.* Role of hedgehog signaling in ovarian cancer. *Clin Cancer Res* **14**, 7659-7666 (2008).
39. Liao, X. *et al.* Aberrant activation of hedgehog signaling pathway in ovarian cancers: effect on prognosis, cell invasion and differentiation. *Carcinogenesis* **30**, 131-140 (2009).
40. Li, Y., Wang, S., Ni, H.M., Huang, H. & Ding, W.X. Autophagy in alcohol-induced multiorgan injury: mechanisms and potential therapeutic targets. *Biomed Res Int* **2014**, 498491 (2014).
41. Mauvezin, C. & Neufeld, T.P. Bafilomycin A1 disrupts autophagic flux by inhibiting both V-ATPase-dependent acidification and Ca-P60A/SERCA-dependent autophagosome-lysosome fusion. *Autophagy* **11**, 1437-1438 (2015).
42. Ding, A.X. *et al.* CasExpress reveals widespread and diverse patterns of cell survival of caspase-3 activation during development in vivo. *Elife* **5** (2016).
43. Sun, G. *et al.* A molecular signature for anastasis, recovery from the brink of apoptotic cell death. *J Cell Biol* **216**, 3355-3368 (2017).
44. Mille, F. *et al.* The Patched dependence receptor triggers apoptosis through a DRAL-caspase-9 complex. *Nat Cell Biol* **11**, 739-746 (2009).
45. Fombonne, J. *et al.* Patched dependence receptor triggers apoptosis through ubiquitination of caspase-9. *Proc Natl Acad Sci U S A* **109**, 10510-10515 (2012).
46. Liang, Y.Y. *et al.* dSmurf selectively degrades DPP-activated MAD and its overexpression disrupts imaginal disc development. *J Biol Chem* (2003).

47. Martin, D.N. & Baehrecke, E.H. Caspases function in autophagic programmed cell death in Drosophila. *Development* **131**, 275-284 (2004).
48. Daish, T.J., Mills, K. & Kumar, S. Drosophila caspase DRONC is required for specific developmental cell death pathways and stress-induced apoptosis. *Dev Cell* **7**, 909-915 (2004).
49. Fadeel, B. & Orrenius, S. Apoptosis: a basic biological phenomenon with wide-ranging implications in human disease. *J Intern Med* **258**, 479-517 (2005).
50. Moreno, E., Basler, K. & Morata, G. Cells compete for decapentaplegic survival factor to prevent apoptosis in Drosophila wing development. *Nature* **416**, 755-759 (2002).
51. Williams, D.W. & Truman, J.W. Remodeling dendrites during insect metamorphosis. *Journal of neurobiology* **64**, 24-33 (2005).
52. Huey, R.B., Wakefield, T., Crill, W.D. & Gilchrist, G.W. Within- and between-generation effects of temperature on early fecundity of Drosophila melanogaster. *Heredity (Edinb)* **74 (Pt 2)**, 216-223 (1995).
53. Terashima, J. & Bownes, M. Translating available food into the number of eggs laid by Drosophila melanogaster. *Genetics* **167**, 1711-1719 (2004).
54. Terashima, J., Takaki, K., Sakurai, S. & Bownes, M. Nutritional status affects 20-hydroxyecdysone concentration and progression of oogenesis in Drosophila melanogaster. *J Endocrinol* **187**, 69-79 (2005).
55. Pepling, M.E. Hedgehog signaling in follicle development. *Biol Reprod* **86**, 173 (2012).
56. Zhou, J., Peng, X. & Mei, S. Autophagy in Ovarian Follicular Development and Atresia. *Int J Biol Sci* **15**, 726-737 (2019).
57. Dick, S.A. & Megeney, L.A. Cell death proteins: an evolutionary role in cellular adaptation before the advent of apoptosis. *Bioessays* **35**, 974-983 (2013).
58. Lee, R.E., Brunette, S., Puente, L.G. & Megeney, L.A. Metacaspase Yca1 is required for clearance of insoluble protein aggregates. *Proc Natl Acad Sci U S A* **107**, 13348-13353 (2010).
59. Hurst, P.R., Mora, J.M. & Fenwick, M.A. Caspase-3, TUNEL and ultrastructural studies of small follicles in adult human ovarian biopsies. *Hum Reprod* **21**, 1974-1980 (2006).
60. Zeng, X. & Ju, D. Hedgehog Signaling Pathway and Autophagy in Cancer. *Int J Mol Sci* **19** (2018).
61. Song, X. *et al.* Activation of hedgehog signaling and its association with cisplatin resistance in ovarian epithelial tumors. *Oncol Lett* **15**, 5569-5576 (2018).
62. Zhu, L. *et al.* Autophagy is a pro-survival mechanism in ovarian cancer against the apoptotic effects of euxanthone. *Biomed Pharmacother* **103**, 708-718 (2018).
63. Yang, C. & Novack, D.V. Anti-cancer IAP antagonists promote bone metastasis: a cautionary tale. *J Bone Miner Metab* **31**, 496-506 (2013).
64. Schneider, C.A., Rasband, W.S. & Eliceiri, K.W. NIH Image to ImageJ: 25 years of image analysis. *Nat Methods* **9**, 671-675 (2012).
65. Buszczak, M. *et al.* The carnegie protein trap library: a versatile tool for Drosophila developmental studies. *Genetics* **175**, 1505-1531 (2007).

842

843

844

CONTRIBUTIONS

L.A.B-L. was responsible for the initial conception of the work and original writing of the manuscript. The experimental design was elaborated by A.G and L.A.B-L. A.G was responsible for most of the experimental work. D.I. performed some experiments under the supervision of A.G. The figure preparation was made by A.G and L.A.B-L. All co-authors have provided useful criticisms and commented on the manuscript before submission.

ACKNOWLEDGEMENTS

Thanks for providing flies and reagents to; Isabel Guerrero (*ptc*-GFP; Centro de Biología Molecular); Pascal Meier (UAS-*Dronc*-RNAi, UAS-*Drice*-RNAi, UAS-*Dcp*-RNAi, UAS-*Damm*-RNAi and UAS-*Decay*-RNAi); Alex Gould (anti-Castor antibody, CRICK Institute) and the Developmental Studies Hybridoma Bank (antibodies), Addgene (pCDNA3-connexin-GFP-Apex2 plasmid), Bloomington Stock Center (fly strains), Kyoto Stock Center (fly strains) and DGRC (wild-type cDNA of *dronc*). Thanks to Genewiz and Bestgene for making the DNA synthesis and generating the transgenic flies, respectively. Thanks also to Ulrike Gruneberg, Sonia Muliyil, Xavier Franch-Marro, Jordan Raff and the caspaselab members (https://www.caspaselab.com) for the critical reading of the manuscript and valuable suggestions. This work has been supported by Cancer Research UK C49979/A17516 and the John Fell Fund from the University of Oxford 162/001. L.A.B-L. is a CRUK Career Development Fellow (C49979/A17516) and an Oriel College Hayward Fellow. A.G. is a postodoctoral fellow of CRUK (C49979/A17516).

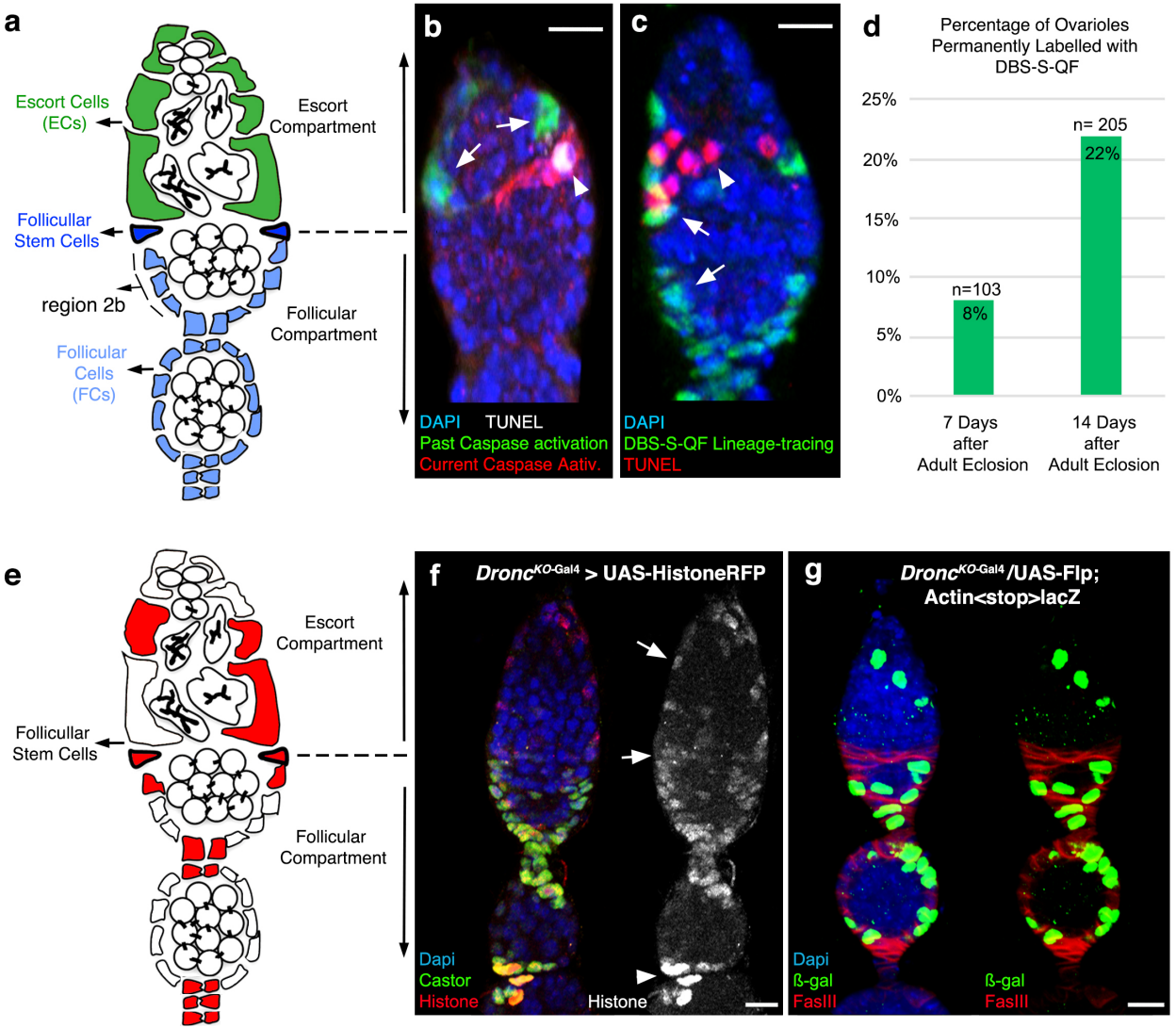

Galasso et al Figure 1

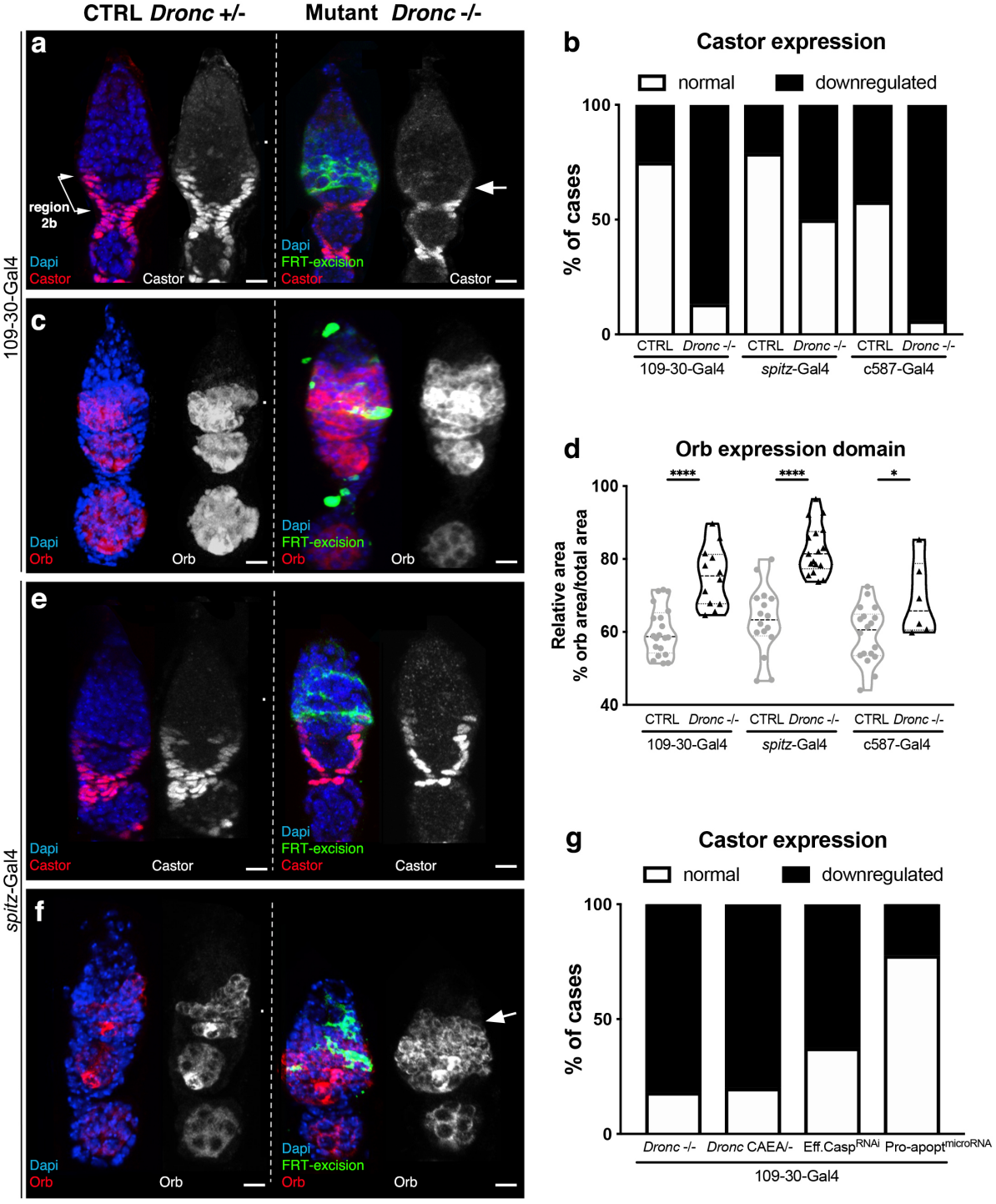

Galasso et al Figure 2

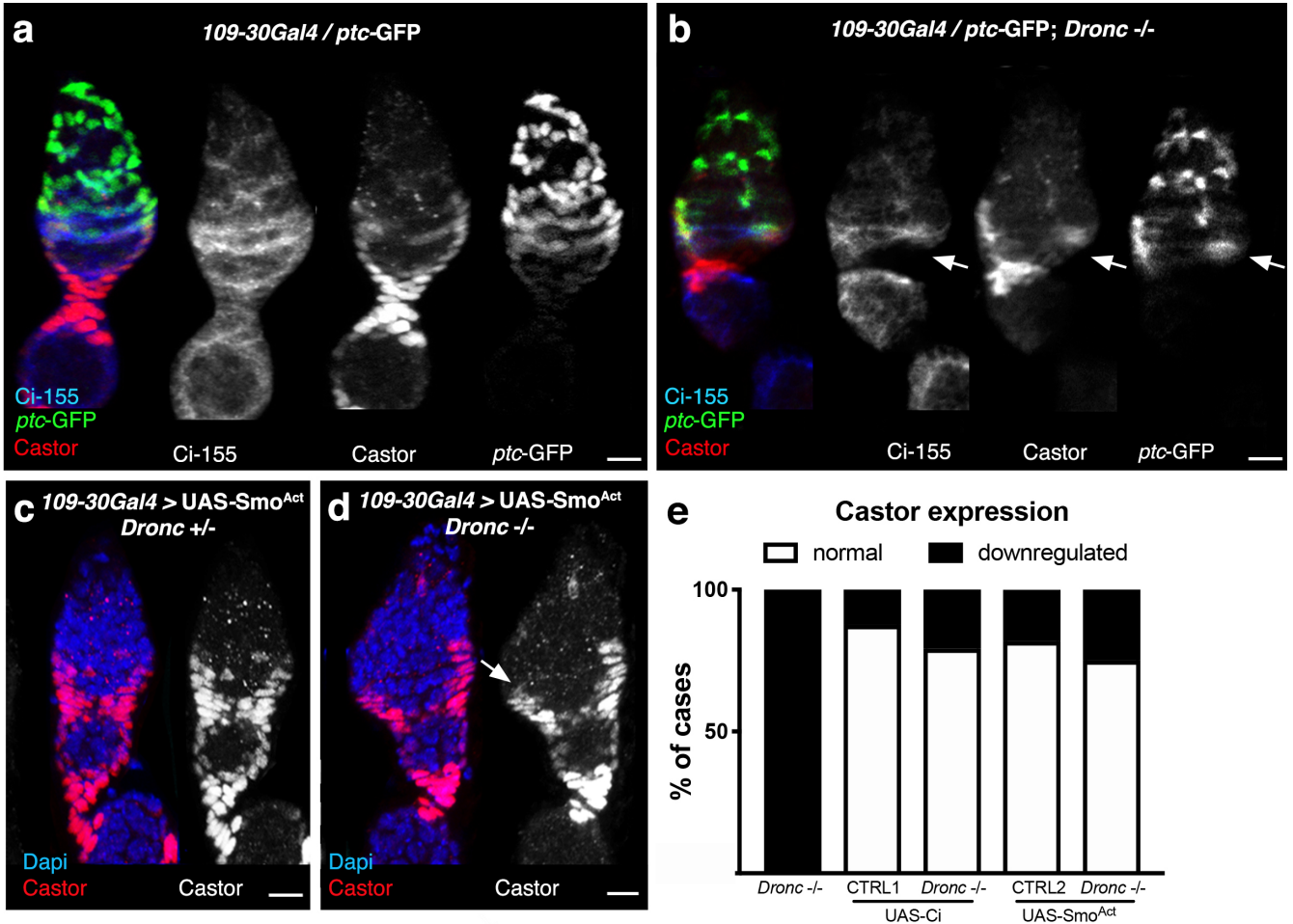

Galasso et al Figure 3

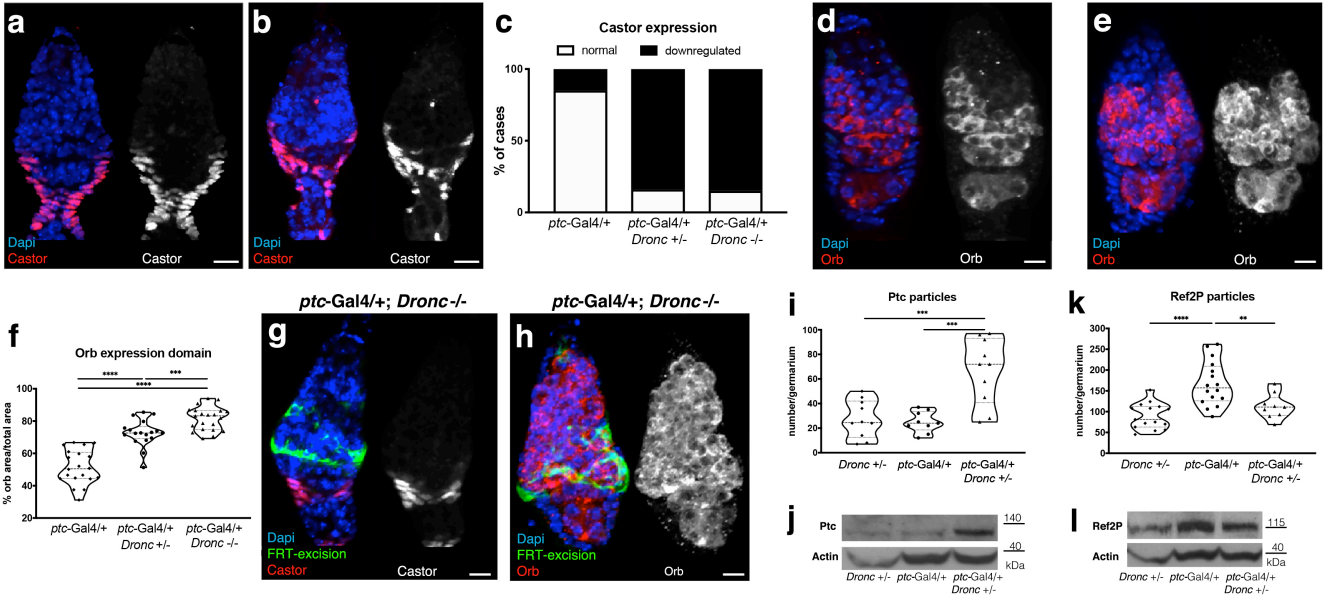

Galasso et al Figure 4

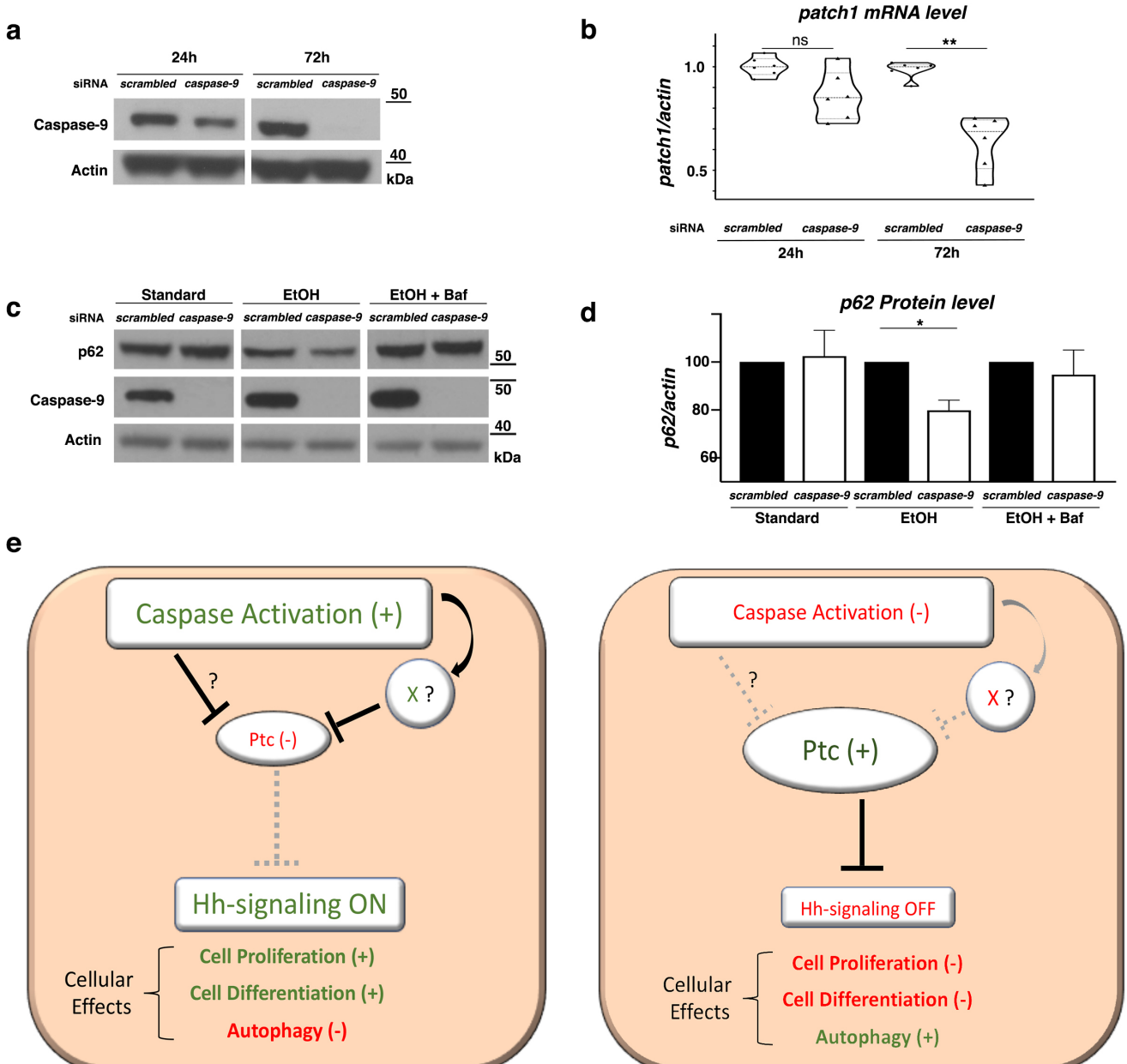

Galasso et al Figure 5